ACS Synthetic Biology

Article

New intracellular shikimic acid biosensor for monitoring shikimate synthesis in *Corynebacterium glutamicum*

Chang Liu, Bo Zhang, Yi-Ming Liu, Keqian Yang, and Shuang-Jiang Liu

ACS Synth. Biol., **Just Accepted Manuscript** • DOI: 10.1021/acssynbio.7b00339 • Publication Date (Web): 31 Oct 2017

ACS Publications

ACS Synthetic Biology is published by the American Chemical Society. 1155 Sixteenth Street N.W., Washington, DC 20036

New intracellular shikimic acid biosensor for monitoring shikimate synthesis in *Corynebacterium glutamicum*

Chang Liu[1, 2], Bo Zhang[1, 3], Yi-Ming Liu[1], Ke-Qian Yang[1†], Shuang-Jiang Liu[1*]

[*]Correspondence: liusj@im.ac.cn

[†]Co-correspondence, deceased March 21st, 2017

[1]State Key Laboratory of Microbial Resources, Institute of Microbiology,

Chinese Academy of Sciences, West Beichen Road No.1, 100101 Beijing, PR China.

[2]University of Chinese Academy of Sciences, 100101 Beijing, PR China.

[3]Zhejiang University of Technology, 310014 Hangzhou, PR China.

Abstract

The quantitative monitoring of intracellular metabolites with *in vivo* biosensors provides an efficient means of identifying high-yield strains and observing product accumulation in real time. In this study, a shikimic acid (SA) biosensor was constructed from a LysR-type transcriptional regulator (ShiR) of *Corynebacterium glutamicum*. The SA biosensor specifically responded to the increase of intracellular SA concentration over a linear range of 19.5 ± 3.6 to 120.9 ± 1.2 fmole at the single-cell level. This new SA biosensor was successfully used to 1) monitor the SA production of different *C. glutamicum* strains; 2) develop a novel result-oriented high-throughput ribosome binding site screening and sorting strategy that was used for engineering high-yield shikimate-producing strains; and 3) engineer a whole-cell biosensor through the co-expression of the SA sensor and a shikimate transporter *shiA* gene in *C. glutamicum* RES167. This work demonstrated that a new intracellular SA biosensor is a valuable tool facilitating the fast development of microbial SA producer.

Keywords: shikimic acid biosensor, *Corynebacterium glutamicum*, transcriptional regulator, single-cell sorting, high-throughput screening, whole-cell biosensor

Introduction

Biosensors can be classified into four categories based on their sensing and reporting mechanisms: 1) transcriptional factor (TF)-based biosensors; 2) riboswitch biosensors; 3) biosensors based on protein interactions (such as fluorescence resonance energy transfer system); and 4) biosensors based on artificial proteins or proteins with specific functions[1-3]. Currently, TF-based biosensors are the most widely used due to the prevalence of prokaryotic TFs that can detect a wide variety of metabolites. TF-based biosensors have been applied in the high-throughput screening of engineered bacteria[3-5], fast selection of desirable mutations[6, 7] and dynamic regulation of synthetic pathways[6, 8, 9]. Recently, such biosensors have also been used in the adaptive evolution of bacterial strains[10] and real-time monitoring of metabolites[11-13].

Shikimic acid (SA) is a metabolic intermediate of the shikimate pathway (Figure 1), an important primary metabolic pathway leading to the biosynthesis of aromatic amino acids and secondary metabolites such as lignin[14] and alkaloids[15]. SA is also used for the chemical synthesis of Oseltamivir[16]. Microbial production of SA has been realized with engineered strains of *Escherichia coli*[16, 17], *Bacillus subtilis*[18, 19], and *Corynebacterium glutamicum*[20, 21]. Genetic disruption of the shikimate pathway at the downstream of shikimic acid has been commonly used to generate shikimate-accumulating strains[22-24] (Figure 1), and further rational engineering of metabolic networks in shikimate-accumulating strains has been applied to obtain highly productive strains[20, 25-29]. However, the development of productive bacterial strains using genetic, biochemical or rational engineering strategies is often restricted

by 1) the limited knowledge of quantitative description of the complex bacterial physiological status and metabolic network fluxes and 2) the low efficiency of genetic manipulations and tedious workload required to identify high-yield strains from huge numbers of mutants[3, 30, 31]. Recently, intracellular biosensors have emerged as a promising tool to overcome these obstacles[3], and many TF-based biosensors have been applied in engineering the production of high-value products such as amino acids[5, 30], aromatic compounds[32], organic acids[33-35], alcohols[36] and other microbial synthesized chemicals[37, 38]. Given that SA is a key metabolic intermediate that networks with many cellular processes and is also a commercially important product, the development of an SA-specific biosensor is of practical importance.

In this study, a novel SA biosensor was designed and constructed based on the LysR-type transcriptional regulator ShiR from *C. glutamicum*[39]. The newly constructed SA biosensor was characterized and used to monitor SA production in *C. glutamicum* strains in real time. In combination with a fluorescence-activated cell sorting (FACS) approach, the SA biosensor was successfully applied in the high-throughput screening of high-yield SA-producing strains. In addition, this biosensor was further used to detect extracellular shikimate when a shikimate transporter (*shiA*) gene was co-expressed with the SA sensor in *C. glutamicum*.

Results and Discussion

Design and construction of an SA biosensor based on a LysR-type transcriptional regulator

The biosensor was designed using a recently reported LysR-family transcriptional

regulator, ShiR (CgR2524, NCBI Reference Sequence: WP_003863076.1), and its cognate binding region, i.e., the putative promoter region of the *shiA* gene (CgR2523, NCBI Reference Sequence: WP_011897860.1)[39]. To construct the SA biosensor, the putative *shiA* promoter was chemically synthesized and was placed in front of the *eGFP* gene. The promoter-*eGFP* fusion was subsequently cloned into the plasmid pEC99-lacI^{q-} to obtain the biosensor plasmid pSA (Table 1). Considering that the *shiR* constitutively expressed in *C. glutamicum*[39], the *shiR* gene was not further cloned onto the pSA for overexpression. The working principle of the intracellular SA biosensor is illustrated in Figure 2a. In the absence of SA molecules, ShiR binds to the target promoter region and impedes the transcription of *eGFP* gene (Figure 2a), resulting in no fluorescence signal being generated. When the SA exists and binds to ShiR as an effector, the ShiR-SA complex will activate the transcription of the *eGFP* gene, leading to its subsequent translation and the production of fluorescence signals (Figure 2b). The functionality of biosensor was then tested by microscopy in *C. glutamicum*. The pSA was transformed into the SA-accumulating strain Δ*aroK* to obtain the strain LSA and the non-SA-accumulating strain RES167 to obtain the strain SENSOR, respectively. The *shiR* on chromosome expressed constitutively in both strains while the intracellular SA only accumulated constantly in strain LSA. The fluorescent signals of two strains were detected using a confocal laser scanning microscopy. As shown in Figure 2c and 2d, the LSA cells displayed much stronger fluorescence in comparison to the SENSOR cells after incubation for 24 hours, demonstrating that the biosensor worked well in *C. glutamicum* as the increase of

intracellular SA was converted into the enhancement of fluorescent outputs.

The responsive specificity of the SA biosensor was characterized *in vivo*. Unlike TetR- or MarR-family TF regulating downstream gene transcription by binding to or dissociating from cognate DNA sequence in terms of whether the effector is present[40, 41], the LysR-family TF binds to its cognate DNA region all the time and regulates gene transcription by conformational change[42]. Therefore, the binding specificity of ShiR, a LysR-type TF, cannot be characterized using the *in vitro* EMSA (Electrophoretic Mobility Shift Assay)[39, 43]. As an alternative, an *in vivo* approach for characterization of the biosensor specificity was developed based on the sole-carbon-source culture experiment performed by Kubota et al[39]. To identify whether the constructed biosensor specifically responds to SA, the SENSOR strain was cultured using SA and its analogues that would present in *C. glutamicum* during SA production (listed in the legend of Figure S1) as sole carbon source, and the bacterial growth (OD_{600nm}) as well as the fluorescence intensity (FI) was monitored during cultivation. As shown in Figure S1a, though the SENSOR cells grew badly with SA as sole carbon source, the relative fluorescence intensity (RFI) increased after incubation for 24hours, while for the other tested chemicals, the SENSOR cells grew well but the RFI did not increase with time. The results revealed that none of the tested substrates, except for SA, can activate the fluorescent response of biosensor.

The SA biosensor responded to intracellular SA

To further quantify the functionality of the intracellular biosensor, the plasmid pSA was

then transformed into a high-SA-accumulating strain *C. glutamicum* GBTDE[21], derived by introducing a SA synthesis module into Δ*aroK* (Table 1), to obtain the new strain HSA, and the response of SA biosensor to the intracellular shikimate accumulation was monitored during fermentation. The HSA strain was cultured in Medium B for 13 hours to the late log phase (Figure S2) before the overexpression of SA synthesis module was initiated by IPTG. The time point when IPTG was added to the culture was recognized as the starting time for SA fermentation ("hour 0" in Figure 3). The RFIs and the intracellular SA concentrations were measured with time, and the results were shown in Figure 3a.The intracellular SA concentration and RFI at time 0 was 19.5 ± 3.6 fmole/cell and 212 ± 11 (FI/OD_{600nm}), respectively. From 0-6 hours, the RFI increased as the SA accumulated and the intracellular SA concentration reached a maximum value of 120.9 ± 1.2 fmole/cell at hour 6 and started to decrease drastically to 36.1 ± 3.1 at hour 11. However, it was surprising to observe that the RFI reached its peak value of 722 ± 27 (FI/OD_{600nm}) at hour 7, one-hour-lagging to the saturation of intracellular SA. After that, the RFI slightly declined to 635 ± 55 at hour 8 and remained relatively stable from 8 to 11 hours. Further regression analysis revealed that the RFI linearly responded to the intracellular SA concentration with one-hour lag (shown in Figure 3b). Namely, the RFIs from 1-7 hours linearly responded to the cytosolic SA accumulation from 0-6 hours and the linear response range of the SA biosensor to intracellular SA was from19.5 ± 3.6 to 120.9 ± 1.2 fmole/cell. After that, though the SA concentration sharply decreased, the RFIs remained stable rather than responded to the SA reduction.

So far as we know, it was the first time to report such output-delay phenotype of a TF-based biosensor, of which the causations could be complicated and unclear yet. It probably related to the existence of rise-time[44] and transcriptional delay[45] in cell regulation networks, or might be due to the time required for translation and protein maturation[46]. Moreover, it was found that the novel SA biosensor could sensitively respond to the increase of SA concentration but not to its decrease, which seemed to be logical since the removal of SA from TF-effector complex and the clearance of existed transcripts and florescent proteins needed time[47, 48 49].

In summary, the above results suggested that the SA biosensor could be applied for quantification of the increase of intracellular SA at concentrations ranging from 19.5 ± 3.6 to 120.9 ± 1.2 fmole/cell. Noticeably, the detection range of the biosensor to the intracellular SA is strain-dependent as the 120.9 ± 1.2 fmole is the maximum concentration that the intracellular SA can reach in a *C. glutamicum* cell and due to which whether the biosensor responds to SA concentrations higher than 120.9 fmole cannot be determined in *C. glutamicum.* If the biosensor will be further used in other bacteria species, re-characterization of the strain-dependent detection range is obligatory.

The SA biosensor is applicable for monitoring SA production in *C. glutamicum*

The applicability of biosensor in real-time monitoring of SA production in SA producers was validated. The biosensor was transformed into three SA producers to obtain LSA (low-productivity), MSA (mid-productivity) and HSA (high-productivity), respectively

(see table 1). Three strains were separately cultured to the late-log phase and the SA fermentation was initiated by adding 1mM IPTG to the cultures. The culture broth was sampled regularly since then. As shown in Figure 4a, the final SA titers in medium broths of LSA, MSA and HSA strains were 1.55 ± 0.06, 3.96 ± 0.23 and 16.41 ± 0.75 mM, respectively. The correlation analysis (Figure 4b) showed that the RFIs of the LSA and MSA strains were linearly correlated with their SA titers over the entire fermentation period (0-52 hours), whereas for the high-yield strain HSA, the RFIs partially responded to the increase in SA titers from 0 to 7 hours. Specifically, as the SA titers increased from 0.50 ± 0.07 mM at hour 0 to 4.24 ± 0.23 mM at hour 7, the RFIs increased correspondingly demonstrating a linear response to the increased SA titers. After 7 hours, the RFI remained at a constant level without further increase. In conclusion, the SA biosensor was applicable for real-time monitoring of SA production in different *C. glutamicum* producers as long as the titer was below 4.24 ± 0.23 mM. Actually, when we used the biosensor to monitor SA production, we essentially still monitored the change of intracellular SA concentration within the SA producer, only that the increase of intracellular SA in cells correlated with the increase of SA titer in broth. Once the cytoplasmic SA reached the maximum concentration and declined afterwards, the positive correlation between intracellular and extracellular SA disappeared, and the fluorescence could not reflect the increase of SA titer anymore. Given that SA is a key intermediate of the shikimate pathway, which networks with many cellular processes, the development of an SA-specific, on-line monitoring approach is of practical importance.

Application of the SA biosensor in single-cell sorting and high-throughput screening of an RBS library for a high-yield *C. glutamicum* strain

In addition to monitoring SA production, we also used the new SA biosensor to screen for high-yield *C. glutamicum* strains at the single-cell level. To achieve this, a high-throughput sorting method based on the SA biosensor was established. The efficiency of the SA biosensor-based FACS approach was evaluated using a mixture of HSA and LSA cells. As shown in Figure 5, two distinct cell populations (I and II) were separated in terms of fluorescence intensity. Cells with top 50% strongest fluorescence in population II were sorted into 96-well plate for cultivation, and their identities were determined by PCR amplification of a targeted DNA fragment. The results showed that 94 out of 96 cells were HSA cells, representing a fairly high sorting accuracy.

The *tktA* gene encodes a transketolase that catalyzes the formation of E4P, a direct precursor of the shikimate pathway (see Figure 1), and overexpression of *tktA* has been used as an efficient metabolic engineering strategy to improve SA production[20]. Gene expression in bacteria is commonly controlled using promoters, besides that, a relatively overlooked cis element is RBS which has been shown to have a strong influence on translation strength[21, 50]. Though increasing studies have used RBS as a regulatory tool in tuning genetic circuits, precise selection of an optimal RBS from a large-scale library for the target gene is still a challenge[21, 51, 52]. In this work, the biosensor-based FACS approach was used to screen a *tktA* RBS library to optimize gene expression for SA production. To obtain high-yield *C. glutamicum* strains, the RLIB cells (strain LSA harboring t*ktA* RBS library pRLIB, Table 1) were induced with

IPTG for 27 hours to overexpress the *tktA* gene under control of different RBSs and screened by flow cytometry (Figure 6a). The LSA was used as a negative control, and the RLIB cells having stronger fluorescence than the control group were considered to be positive. To reduce false positive cells, two rounds of pre-sorting and a final sorting step were performed (Figure 6b-6d). The sorted single cells were cultivated in a 96-well plate. After further incubation and induction of these sorted cells, the fluorescence of each strain was measured, and the results were presented in Figure 6e. Three strains (strains 13, 22 and 23) with the strongest FI were chosen for scaled-up fermentation in 500-mL flasks. The TKTA strain harboring an overexpressed *tktA* gene controlled by a strong RBS (designated as RBS_u; Table 1) was used as the positive reference, while the LSA strain was used as the negative control. As shown in Figure 6f (the bar chart), strain 22 had the highest SA yield. Compared with strain TKTA, the SA titer of strain 22 increased 90% to 3.72 ± 0.35 mM, a more than 2.4-fold improvement over the LSA strain. These results validated the applicability of the biosensor-based FACS approach in developing an SA high-yield *C. glutamicum* strain. Such high-throughput screening strategy enabled fast selection of high SA production mutants without much concern for the engineering strategy or workload.

The *tktA* RBS sequences of strains TKTA, 13, 22, and 23 were listed in Figure 6g, and the RBS sequence from strain 22 was considered to be the optimal RBS for *tktA* overexpression in *C. glutamicum* for SA production purposes. To quantitatively characterize the strengths of the obtained RBSs, four plasmids for expression of the

RBS-tktA-egfp fusion were constructed (designated $pRBS_u$-TE, $pRBS_{13}$-TE, $pRBS_{22}$-TE, and $pRBS_{23}$-TE,). The *tktA-egfp* fusion without an RBS sequence (designated pTE) was used as a negative control. The constructed plasmids were expressed in *C. glutamicum* RES167, and the RFIs were measured and are shown in the line chart of Figure 6f, which clearly indicated that the strength of RBS_{13} and RBS_{23} was one-fifth of the RBS_u's , while the RBS_{22} was one-third of RBS_u. As we known, the optimal RBS for a specific gene should have a ribosome-recruiting rate identical to (or slightly below) the slowest rate at which the ribosomes pass through the codons of mRNA[20, 53, 54]. Therefore, translational over-initiation mediated by over-strong RBS would cause an additional burden or detriment to cells, and should be prevented during RBS engineering. The biosensor-based FACS method was validated to be an effective and precise strategy for RBS optimization, as it enabled the result-oriented *in situ* screening of the best-fit RBS sequence for the target gene in consideration of the complex cellular physiology and orthogonality of the genetic networks. A similar top-down screening strategy may also work for the selection of optimal promoters, terminators and other regulatory parts. In fact, due to the complexity of physiology, the traditional bottom-up design-based engineering strategy runs into a stone wall at times. Alternatively, the biosensor-based high-throughput engineering strategy enabled the optimal combination of genetic parts to be achieved without comprehensive knowledge of each individual part, which was obviously more efficient[55, 56].

Construction of a whole-cell biosensor for extracellular SA detection by engineering the *in vivo* SA biosensor

According to the results of the biosensor-specificity experiment (Figure S1a), the SENSOR strain hardly grew with the supplemented SA as sole carbon source. Bioinformatics analysis of the *C. glutamicum* ATCC13032 genome revealed that this parent strain of RES167 lacked a *shiA* gene, which was found in other strains as *C. glutamicum* R^{39} to encode a shikimate transporter for transportation of extracellular SA into the cytoplasm. Considering this, a *shiA* expression cassette was constructed and inserted into the pSA plasmid to obtain the novel plasmid pWCSA (Figure 7). The pWCSA plasmid was then transformed into *C. glutamicum* RES167 to obtain the strain WCSENSOR, which was further characterized by its response to extracellular SA as well as other carbon sources. As shown in Figure S1b, the WCSENSOR was able to grow well using SA as sole carbon source and response specifically to SA. Then, the dose response of WCSENSOR cells to extracellular SA concentrations of 0 to 900 mM (pH 7.4) was characterized. The responsive range of WCSENSOR cells to the supplemented SA concentration was from 0 to 500 mM, while the RFI of WCSENSOR cells began to decrease when the SA concentration exceeded 500 mM (Figure S3). Further regression analysis of the response curve revealed that the RFIs of WCSENSOR cells logarithmically correlated with extracellular SA concentrations ranging from 0 to 500 mM (Figure 8a), while the linear detection range of the whole-cell biosensor was further experimentally determined to be between 1 and 100 mM as shown in Figure 8b. In summary, by introducing a shikimate transporter into the SA biosensor plasmid, the *C. glutamicum* cells harboring the modified biosensor

could respond to external SA and thus, can be used as a whole-cell biosensor to detect extracellular SA over a wide dynamic range, which can be further applied in many research fields, such as environment monitoring and bioengineering[57-60].

A most recent publication reported an *Escherichia coli*-based whole-cell SA biosensor constructed by mutagenesis of the uric acid-responsive regulatory protein, which was successfully applied in analyzing and engineering the metabolic flux of shikimate pathway in *E. coli*[61]. However, there are many differences between our work and theirs, regarding the biosensor-constructing strategy, detection range, screening approach, bacterial chassis and applicable fields. Firstly, we constructed an intracellular biosensor that specifically responded to intracellular SA and then developed an additional whole-cell biosensor to sense extracellular SA based on it, while the reported biosensor was a whole-cell biosensor; Secondly, our novel whole-cell biosensor has a way boarder detection range (0-500 mM) in comparison to the reported one of which the responsive range to external SA was 0-20 mM; Thirdly, our intracellular SA biosensor enabled a high-throughput FACS-based single cell screening approach, while the recent published work screened mutants by visually comparing the color variations among colonies. Given that the number of single colony on one plate is generally about 100-1,000 (only the colonies on the same plate are comparable) while over 10,000 single cell can be screened by FACS per minute and over 10^5 cells were collected in each sorting step, the FACS-based screening approach is apparently a more high-throughput and time-saving screening strategy; Fourthly, instead of *E. coli*, we used the *C. glutamicum* as the chassis for

characterization and proof-of-principle application of biosensor, because the *C. glutamicum,* as an important GRAS (Generally Recognized as Safe) industrial bacterium, is a more promising SA producer deserving more attention and further improvement; Finally, besides of metabolic engineering of shikimate pathway, our study has broadened the applicable fields of SA biosensor to fast development of SA high-yield strain, resulted-orientated optimization of regulatory parts such as RBS, real-time monitoring of SA production, and environmental SA detection.

Methods

Bacterial strains, media and growth conditions

The bacterial strains and plasmids used in this study are listed in Table 1. *E. coli* and *C. glutamicum* were cultivated as previously described[21]. When needed, chloramphenicol and kanamycin were used at final concentrations of 10 and 25 μg/mL, respectively. The SA production of different *C. glutamicum* strains was carried out in 500-mL flasks containing 100 mL of medium B[21]. Each strain was inoculated and incubated for 13 hours to reach a late-log phase and (if necessary) 1 mM of isopropyl β-D-1-thiogalactopyranoside (IPTG) was added to the culture to initiate the overexpression of SA synthesis modules as pGBTDE and pGBD9, the *tktA* RBS library pRLIB or other targeted genes as *tktAs* and *tktA-eGFP* fusions under control of different RBSs. The time point when the IPTG was added to the culture was recognized as the starting time for fermentation or SA production. The RBS strength assay and dose-response experiments of the SA whole-cell biosensor were

performed in MS medium[21] with or without 0.2% sucrose. Competent cells were prepared and electro-transformed following a previously reported protocol[62].

DNA manipulations

The plasmid pEC99-*lacI*$^{q-}$ was derived from pEC-XK99E[21] by replacing the promoter P_{tac}, the *rrnB* T1T2 terminator and the *lacI*^{q} promoter with the Biobrick adapter[63] by PCR (primer pair: P_99-*lacI*$^{q-}$_F and P_99-*lacI*$^{q-}$_R, Table 1) and Gibson assembly (NEB, the United Kingdom). The promoter region to which ShiR binds (see Table 1), *eGFP* (NCBI accession number: AFA52654.1), and the *rrnB* T1T2 terminator region, designed to carry the standard Biobrick cutting sites, were synthesized (GENEWIZ Inc., China) and ligated into pEC99-*lacI*$^{q-}$ using Biobrick assembly[63] to obtain the pSA plasmid (Figure 1). The pBiobrick19 vector was derived from pXMJ19[21] by replacing the expression cassette (promoter P_{tac}, the *rrnB* T1T2 terminator) with the Biobrick adapter using PCR (primer pair: P_ pB19_F and P_ pB19_R, Table 1) and Gibson assembly (NEB, the United Kingdom). The *tktA* sequence (NCgl1512, NCBI accession number: NP_600788.1) was synthesized to retain the Biobrick adapter and a strong RBS sequence (AAAGGAGTTGCTT) and was subsequently cloned into pBiobrick19 to obtain the pTKTA plasmid. The plasmid pWCSA was constructed by the insertion of a *shiA* expression cassette, containing a synthesized *shiA* gene (NCBI Reference Sequence: WP_011897860.1) under regulation of the constitutive promoter P_{4945} (the sequence is shown in Table 1) with a terminator (the sequence is shown in Table 1), into the pSA plasmid.

Confocal laser scanning microscopy

The glass slabs with bacteria were examined using a LEICA TCS SP8 confocal microscope (Leica Microsystems, Germany) with a 60 x oil objective. The emission wavelengths were from 499-542 nm, and the excitation wavelength used was 488 nm. The images were taken under one X-Y plane.

Measurement of fluorescence intensity of *C. glutamicum* cells

To measure the fluorescence intensity (FI), the *C. glutamicum* cells were suspended in MS medium[21] and transferred into a 96-well plate, then were scanned using a BioTek® synergy H4 Hybrid Reader (BioTek Instruments, Inc, USA) with an excitation wavelength of 488 nm, an emission wavelength of 509 nm and a sensitivity parameter of 75. In addition, the 96-well plate was also scanned at 600 nm to determine the optical density (OD) of the cell samples. Relative fluorescence intensity represents the fluorescence intensity per unit optical density of cells (FI/ OD_{600nm}). All the values shown were the means of duplicates.

Characterization of the intracellular biosensor specificity

The specificity assay was developed from the previous reported sole-carbon-source culture experiment[39]. The strain SENSOR or WCSENSOR was incubated in MS medium with 20 mM of quinic acid (QA), protocatechuate (PCA), 3-dehydroshikimate (DHS), 3-dehydroquinate (DHQ), shikimic acid (SA) or sucrose (SUC) as sole carbon source, cells incubated in MS medium without carbon source was used as negative control (BLK). Samples were taken after incubation for 0 hour, 24 hours and 48 hours, and the OD_{600nm} as well as the FI was measured with the method mentioned above.

Measurement of intracellular SA concentration in *C. glutamicum*

The *C. glutamicum* strain HSA was inoculated in medium B with an inoculum size of 1.5% v/v, and incubated for 13 hours to enable the cells to reach a late log phase. Then SA fermentation was started by adding 1 mM IPTG to each culture to induce the expression of shikimate synthesis module pGBTDE. Two milliliter cultures were sampled every hour after fermentation for 0 to 12 hours. Immediately after sampling, the cell pellets were collected by centrifugation at 13,000 rpm for 30 seconds at 4 °C and re-suspended with 100 µl of pre-cooled 20 mM pH 7.4 This-HCl buffer. The cells were then re-collected using a previous reported silicon oil centrifugation approach[64] by replaced the 20% perchloric acid with 50 µl of 20% sucrose solution. The collected cells were stored at -80 °C to cease the cell metabolic activities. To quantify the intracellular SA concentration of cells, each cell sample was re-suspended in 500 µl of 20 mg/ml lysozyme (Amresco, USA), and the cell suspension was treated with ultrasonication for 10 min (set: 20% power, work for 3 s, and stop for 5 s). The cellular lysates were centrifuged at 13000 rpm for 2 min at 4 °C, and the supernatant was collected for further measurement of SA concentration using an HPLC system as described previously[21]. The number of cells was calculated by the plate counting method[65]. Each experiment was performed three times for duplicates.

Monitoring SA production in *C. glutamicum* cultures

The shikimate-producing *C. glutamicum* strains HSA, MSA and LSA were incubated and fermented as depicted previously, and the cultures were sampled regularly during cell growth and fermentation. Samples were centrifuged at 10,000 rpm for 1 min, and the supernatants were stored to measure SA titers using HPLC-based approach[21].

The harvested cells were washed twice with and re-suspended in MS medium. Then, 200 μL of cell suspensions were taken for measurements of FI and OD_{600nm} values using the method described in the previous section. Each experiment was performed three times for duplicates.

Construction of an RBS library for optimization of *tktA* translation during SA production

The *tktA* RBS library (pRLIBs) was synthesized (GENEWIZ, Inc., China) by random mutation of the last eight bases of the reported *tktA* RBS sequence (AAAAGGNNNNNNNN)[21] and was cloned into plasmid pBiobrick19. The RBS library was then transformed into LSA cells to prepare the RLIB cell library for further screening. The RLIB cells were cultivated in BHI medium[21] at 30 °C, at 200 rpm for 4 hours and then inoculated into BHI containing 10 μg/mL chloramphenicol and 25 μg/mL kanamycin for overnight cultivation. To ensure that the RFI of each single cell was comparable, the screening was performed using cells in which the SA concentration was below SA cytoplasmic saturation concentration. Therefore, the proper induction time was determined experimentally. The RLIB cultures were induced with IPTG for set times (from 8 to 40 hours) to determine the optimal induction time. The fluorescence of non-induced cells was defined as the reference, and the enhanced fluorescence from the induced cells was considered to be positive. For each incubation period, 5×10^5 cells were recorded by flow cytometry and the rate of positive fluorescent cells was analyzed. As shown in Figure S4, the proper induction time for the RLIB strain was experimentally determined to be 27 hours since

the highest percentage of positive fluorescent sorted cells was at this time point.

Single-cell sorting with flow cytometry

High-throughput cell screening and sorting was achieved by flow cytometry using a FACS Aria II (BD Biosciences, San Jose, USA), with the excitation and detection wavelengths set at 488 and 530 nm, respectively. The four-way purity mode was used for cell sorting to exclude impurities and non-targeted particles. The threshold rate was 5000 events per second, and sterilized PBS buffer[66] was used as the sheath fluid. The LSA strain was used as a negative control in all flow cytometry experiments. Cells were sorted based on fluorescence enhancement compared to the parental strain. Data were analyzed with the FlowJo FC analysis software 7.6.1.

For single-cell sorting, two rounds of pre-sorting and one round of single-cell sorting were performed to reduce the influence of false positives and random error. The LSA strain was used as a negative control, and RLIB cells with enhanced fluorescence readouts were considered to be positive. For the pre-sorting steps, the RLIB cells, which were pre-induced for a sufficient time in BHI medium, were diluted to 10^7 cells/mL and analyzed by flow cytometry. Approximately 10^5 cells with the top 20% highest fluorescence (10% for the second round of pre-sorting) were separated and collected with 1.5 mL-Eppendorf tubes containing 200 µL of BHI medium. The collected cells were then transferred into a 10-mL glass tube containing 1 mL of BHI medium with kanamycin and chloramphenicol for a 48-hour enrichment growth. The two-round pre-sorted cells were then used for the single-cell sorting. In the final round of sorting, single cells with top 5% highest fluorescence intensities were successively

spotted into a 96-well plate containing 200 μL of BHI medium for a 48-hour cultivation. The single cell in each well of the 96-well plate was cultivated and then inoculated into two 48-well plates with 800 μL of fresh medium B in each well for fermentation. The fermentation cultures were transferred into a 96-well plate for fluorescence screening with the microplate reader mentioned above. Several strains with relatively strong FI were selected for further testing of SA production in 500-mL flasks.

Extracellular SA supplementation experiments

To characterize the response of the biosensor to different concentration of SA supplemented in growth medium, the *C. glutamicum* strains SENSOR and WCSENSOR was inoculated in MS Medium with 2% sucrose and cultured overnight at 30 °C. The overnight culture was then separated into several equal portions according to the SA concentrations designed for dose-response experiments. Each portion of cells was harvested by centrifugation at 6000 rpm for 5 min and was re-suspended in the same volume of MS medium containing a specific concentration of SA (0-900 mM) as the sole carbon source. Three parallel samples were prepared for each SA concentration. The new cultures were aliquoted into a 96-well plate and incubated at 30 °C at 800 rpm for 4 hours. The 96-well plate was scanned with a microplate reader and the RFIs were determined as described above.

Supporting Information

Supplementary Figure S1. The responsive specificity of the constructed biosensor to SA and the growth ability of strain SENSOR and WCSENSOR using SA as sole

carbon source.

Supplementary Figure S2. The growth curves of strain RES167, LSA, MSA and HSA incubated in Medium B.

Supplementary Figure S3. The OD_{600nm} values and the FIs used for characterization of the RFI that responded to the intracellular SA concentrations.

Supplementary Figure S4. The dose response of WCSENSOR cells to extracellular SA concentrations ranging from 0 to 900 mM.

Supplementary Figure S5. FACS-based analysis of the RLIB cultures induced for a different time.

Acknowledgement

We would like to dedicate this paper to Prof. Ke-Qian Yang, who passed away before the paper was submitted. Prof. Yang, an outstanding biologist devoted his life to science, is greatly missed. We thank Ms. Tong Zhao from the Institute of Microbiology Chinese Academy of Sciences for her guidance on the operation of flow cytometry and optimization of FACS-based experiments. We thank Ms. Xiao-Lan Zhang from the Institute of Microbiology Chinese Academy of Sciences for her help in confocal microscopy. We also thank Dr. Wei-Shan Wang and Dr. Ke-Qiang Fan from the Institute of Microbiology Chinese Academy of Sciences, for their scientific advice and discussions. This work was supported by the 973 Project from the Ministry of Science and Technology (No. 2012CB7211-04).

Author Contribution

Chang Liu, Ke-Qian Yang and Shuang-Jiang Liu conceived this project. Chang Liu, Bo Zhang and Yi-Ming Liu designed and accomplished all the experiments. Chang Liu and Shuang-Jiang Liu analyzed the data. Chang Liu, Ke-Qian Yang and Shuang-Jiang Liu wrote the manuscript.

Reference

1. Liu, D., Evans, T., and Zhang, F. (2015) Applications and advances of metabolite biosensors for metabolic engineering, *Metab Eng 31*, 35-43.
2. Michener, J. K., Thodey, K., Liang, J. C., and Smolke, C. D. (2012) Applications of genetically-encoded biosensors for the construction and control of biosynthetic pathways, *Metab Eng 14*, 212-222.
3. Eggeling, L., Bott, M., and Marienhagen, J. (2015) Novel screening methods--biosensors, *Curr Opin Biotechnol 35*, 30-36.
4. Binder, S., Siedler, S., Marienhagen, J., Bott, M., and Eggeling, L. (2013) Recombineering in *Corynebacterium glutamicum* combined with optical nanosensors: a general strategy for fast producer strain generation, *Nucleic Acids Res 41*, 6360-6369.
5. Mustafi, N., Grunberger, A., Kohlheyer, D., Bott, M., and Frunzke, J. (2012) The development and application of a single-cell biosensor for the detection of l-methionine and branched-chain amino acids, *Metab Eng 14*, 449-457.
6. Zhang, J., Jensen, M. K., and Keasling, J. D. (2015) Development of biosensors and their application in metabolic engineering, *Curr Opin Chem Biol 28*, 1-8.
7. Raman, S., Rogers, J. K., Taylor, N. D., and Church, G. M. (2014) Evolution-guided optimization of biosynthetic pathways, *P Natl Acad Sci USA 111*, 17803-17808.
8. Liu, D., Xiao, Y., Evans, B. S., and Zhang, F. Z. (2015) Negative Feedback Regulation of Fatty Acid Production Based on a Malonyl-CoA Sensor-Actuator, *ACS Synth Biol 4*, 132-140.
9. Schendzielorz, G., Dippong, M., Grunberger, A., Kohlheyer, D., Yoshida, A., Binder, S., Nishiyama, C., Nishiyama, M., Bott, M., and Eggeling, L. (2014) Taking Control over Control: Use of Product Sensing in Single Cells to Remove Flux Control at Key Enzymes in Biosynthesis Pathways, *ACS Synth Biol 3*, 21-29.
10. Mahr, R., Gatgens, C., Gatgens, J., Polen, T., Kalinowski, J., and Frunzke, J. (2015) Biosensor-driven adaptive laboratory evolution of l-valine production in *Corynebacterium glutamicum*, *Metab Eng 32*, 184-194.
11. Mustafi, N., Grunberger, A., Mahr, R., Helfrich, S., Noh, K., Blombach, B., Kohlheyer, D., and Frunzke, J. (2014) Application of a Genetically Encoded Biosensor for Live Cell Imaging of L-Valine Production in Pyruvate Dehydrogenase Complex-Deficient *Corynebacterium glutamicum* Strains, *Plos One 9*.
12. Rogers, J. K., Guzman, C. D., Taylor, N. D., Raman, S., Anderson, K., and Church, G. M. (2015) Synthetic biosensors for precise gene control and real-time monitoring of metabolites, *Nucleic Acids Res 43*, 7648-7660.

13. Younger, A. K., Dalvie, N. C., Rottinghaus, A. G., and Leonard, J. N. (2017) Engineering Modular Biosensors to Confer Metabolite-Responsive Regulation of Transcription, *ACS Synth Biol 6*, 311-325.
14. Brown, S. A., and Neish, A. (1955) Shikimic acid as a precursor in lignin biosynthesis.
15. Bochkov, D. V., Sysolyatin, S. V., Kalashnikov, A. I., and Surmacheva, I. A. (2012) Shikimic acid: review of its analytical, isolation, and purification techniques from plant and microbial sources, *J. Biol. Chem 5*, 5-17.
16. Chandran, S. S., Yi, J., Draths, K. M., von Daeniken, R., Weber, W., and Frost, J. W. (2003) Phosphoenolpyruvate availability and the biosynthesis of shikimic acid, *Biotechnol Prog 19*, 808-814.
17. Martinez, J. A., Bolivar, F., and Escalante, A. (2015) Shikimic Acid Production in *Escherichia coli*: From Classical Metabolic Engineering Strategies to Omics Applied to Improve Its Production, *Front Bioeng Biotechnol 3*, 145.
18. Liu, D. F., Ai, G. M., Zheng, Q. X., Liu, C., Jiang, C. Y., Liu, L. X., Zhang, B., Liu, Y. M., Yang, C., and Liu, S. J. (2014) Metabolic flux responses to genetic modification for shikimic acid production by *Bacillus subtilis* strains, *Microb Cell Fact 13*, 40.
19. Licona-Cassani, C., Lara, A. R., Cabrera-Valladares, N., Escalante, A., Hernandez-Chavez, G., Martinez, A., Bolivar, F., and Gosset, G. (2014) Inactivation of pyruvate kinase or the phosphoenolpyruvate: sugar phosphotransferase system increases shikimic and dehydroshikimic acid yields from glucose in *Bacillus subtilis*, *J Mol Microbiol Biotechnol 24*, 37-45.
20. Kogure, T., Kubota, T., Suda, M., Hiraga, K., and Inui, M. (2016) Metabolic engineering of *Corynebacterium glutamicum* for shikimate overproduction by growth-arrested cell reaction, *Metab Eng 38*, 204-216.
21. Zhang, B., Zhou, N., Liu, Y. M., Liu, C., Lou, C. B., Jiang, C. Y., and Liu, S. J. (2015) Ribosome binding site libraries and pathway modules for shikimic acid synthesis with Corynebacterium glutamicum, *Microb Cell Fact 14*, 71.
22. Liu, C., Liu, Y. M., Sun, Q. L., Jiang, C. Y., and Liu, S. J. (2015) Unraveling the kinetic diversity of microbial 3-dehydroquinate dehydratases of shikimate pathway, *AMB Express 5*, 7.
23. Kramer, M., Bongaerts, J., Bovenberg, R., Kremer, S., Muller, U., Orf, S., Wubbolts, M., and Raeven, L. (2003) Metabolic engineering for microbial production of shikimic acid, *Metab Eng 5*, 277-283.
24. Ghosh, S., Chisti, Y., and Banerjee, U. C. (2012) Production of shikimic acid, *Biotechnol Adv 30*, 1425-1431.
25. Escalante, A., Calderón, R., Valdivia, A., de Anda, R., Hernández, G., Ramírez, O. T., Gosset, G., and Bolívar, F. (2010) Metabolic engineering for the production of shikimic acid in an evolved Escherichia coli strain lacking the phosphoenolpyruvate: carbohydrate phosphotransferase system, *Microb Cell Fact 9*, 21.
26. Krämer, M., Bongaerts, J., Bovenberg, R., Kremer, S., Müller, U., Orf, S., Wubbolts, M., and Raeven, L. (2003) Metabolic engineering for microbial production of shikimic acid, *Metab Eng 5*, 277-283.
27. Johansson, L., Lindskog, A., Silfversparre, G., Cimander, C., Nielsen, K. F., and Lidén, G. (2005) Shikimic acid production by a modified strain of E. coli (W3110. shik1) under phosphate-limited and carbon-limited conditions, *Bioeng Biotechnol 92*, 541-552.

28. Shirai, M., Miyata, R., Sasaki, S., Sakamoto, K., Yahanda, S., Shibayama, K., Yonehara, T., and Ogawa, K. (2001) Microorganism belonging to the genus Citrobacter and process for producing shikimic acid, *European Patent 1*.

29. Chandran, S. S., Yi, J., Draths, K., Daeniken, R. v., Weber, W., and Frost, J. (2003) Phosphoenolpyruvate availability and the biosynthesis of shikimic acid, *Biotechnol Progr 19*, 808-814.

30. Binder, S., Schendzielorz, G., Stabler, N., Krumbach, K., Hoffmann, K., Bott, M., and Eggeling, L. (2012) A high-throughput approach to identify genomic variants of bacterial metabolite producers at the single-cell level, *Genome Biol 13*.

31. Dietrich, J. A., McKee, A. E., and Keasling, J. D. (2010) High-throughput metabolic engineering: advances in small-molecule screening and selection, *Annu Rev Biochem 79*, 563-590.

32. Fiorentino, G., Ronca, R., and Bartolucci, S. (2009) A novel *E. coli* biosensor for detecting aromatic aldehydes based on a responsive inducible archaeal promoter fused to the green fluorescent protein, *Appl Microbiol Biotechnol 82*, 67-77.

33. Chen, D. W., Zhang, Y., Jiang, C. Y., and Liu, S. J. (2014) Benzoate Metabolism Intermediate Benzoyl Coenzyme A Affects Gentisate Pathway Regulation in *Comamonas testosteroni*, *Appl Environ Microb 80*, 4051-4062.

34. Ganesh, I., Ravikumar, S., Yoo, I. K., and Hong, S. H. (2015) Construction of malate-sensing *Escherichia coli* by introduction of a novel chimeric two-component system, *Bioprocess Biosyst Eng 38*, 797-804.

35. Tang, S. Y., and Cirino, P. C. (2011) Design and application of a mevalonate-responsive regulatory protein, *Angew Chem Int Ed Engl 50*, 1084-1086.

36. Dietrich, J. A., Shis, D. L., Alikhani, A., and Keasling, J. D. (2013) Transcription factor-based screens and synthetic selections for microbial small-molecule biosynthesis, *ACS Synth Biol 2*, 47-58.

37. Tang, S. Y., Qian, S., Akinterinwa, O., Frei, C. S., Gredell, J. A., and Cirino, P. C. (2013) Screening for enhanced triacetic acid lactone production by recombinant *Escherichia coli* expressing a designed triacetic acid lactone reporter, *J Am Chem Soc 135*, 10099-10103.

38. Siedler, S., Schendzielorz, G., Binder, S., Eggeling, L., Bringer, S., and Bott, M. (2014) SoxR as a single-cell biosensor for NADPH-consuming enzymes in *Escherichia coli*, *ACS Synth Biol 3*, 41-47.

39. Kubota, T., Tanaka, Y., Takemoto, N., Hiraga, K., Yukawa, H., and Inui, M. (2015) Identification and expression analysis of a gene encoding a shikimate transporter of *Corynebacterium glutamicum*, *Microbiol-SGM 161*, 254-263.

40. Ramos, J. L., Martinez-Bueno, M., Molina-Henares, A. J., Teran, W., Watanabe, K., Zhang, X. D., Gallegos, M. T., Brennan, R., and Tobes, R. (2005) The TetR family of transcriptional repressors, *Microbiol Mol Biol R 69*, 326-+.

41. Alekshun, M. N., Levy, S. B., Mealy, T. R., Seaton, B. A., and Head, J. F. (2001) The crystal structure of MarR, a regulator of multiple antibiotic resistance, at 2.3 angstrom resolution, *Nat Struct Biol 8*, 710-714.

42. Schell, M. A. (1993) Molecular-Biology of the Lysr Family of Transcriptional Regulators, *Annu Rev Microbiol 47*, 597-626.

43. Kubota, T., Tanaka, Y., Takemoto, N., Watanabe, A., Hiraga, K., Inui, M., and Yukawa, H.

(2014) Chorismate-dependent transcriptional regulation of quinate/shikimate utilization genes by LysR-type transcriptional regulator QsuR in *Corynebacterium glutamicum*: carbon flow control at metabolic branch point, *Mol Microbiol 92*, 356-368.

44. Rosenfeld, N., Elowitz, M. B., and Alon, U. (2002) Negative autoregulation speeds the response times of transcription networks, *J Mol Biol 323*, 785-793.

45. Gupta, C., Lopez, J. M., Ott, W., Josic, K., and Bennett, M. R. (2013) Transcriptional Delay Stabilizes Bistable Gene Networks, *Phys Rev Lett 111*.

46. Roussel, M. R., and Zhu, R. (2006) Validation of an algorithm for delay stochastic simulation of transcription and translation in prokaryotic gene expression, *Phys Biol 3*, 274-284.

47. Selinger, D. W., Saxena, R. M., Cheung, K. J., Church, G. M., and Rosenow, C. (2003) Global RNA half-life analysis in *Escherichia coli* reveals positional patterns of transcript degradation, *Genome Res 13*, 216-223.

48. Maddocks, S. E., and Oyston, P. C. F. (2008) Structure and function of the LysR-type transcriptional regulator (LTTR) family proteins, *Microbiol-SGM 154*, 3609-3623.

49. Bernstein, J. A., Khodursky, A. B., Lin, P. H., Lin-Chao, S., and Cohen, S. N. (2002) Global analysis of mRNA decay and abundance in *Escherichia coli* at single-gene resolution using two-color fluorescent DNA microarrays, *P Natl Acad Sci USA 99*, 9697-9702.

50. Farasat, I., Collens, J., and Sails, H. M. (2011) Efficient optimization of synthetic metabolic pathways with the RBS Library Calculator, *Abstr Pap Am Chem S 241*.

51. Yi, J. S., Kim, M. W., Kim, M., Jeong, Y., Kim, E. J., Cho, B. K., and Kim, B. G. (2017) A Novel Approach for Gene Expression Optimization through Native Promoter and 5' UTR Combinations Based on RNA-seq, Ribo-seq, and TSS-seq of *Streptomyces coelicolor*, *ACS Synth Biol 6*, 555-565.

52. Nowroozi, F. F., Baidoo, E. E. K., Ermakov, S., Redding-Johanson, A. M., Batth, T. S., Petzold, C. J., and Keasling, J. D. (2014) Metabolic pathway optimization using ribosome binding site variants and combinatorial gene assembly, *Appl Microbiol Biotechnol 98*, 1567-1581.

53. Ceroni, F., Algar, R., Stan, G. B., and Ellis, T. (2015) Quantifying cellular capacity identifies gene expression designs with reduced burden, *Nat Methods 12*, 415.

54. Hersch, S. J., Elgamal, S., Katz, A., Ibba, M., and Navarre, W. W. (2014) Translation initiation rate determines the impact of ribosome stalling on bacterial protein synthesis, *J Biol Chem 289*, 28160-28171.

55. Zhang, F., Carothers, J. M., and Keasling, J. D. (2012) Design of a dynamic sensor-regulator system for production of chemicals and fuels derived from fatty acids, *Nat Biotechnol 30*, 354-359.

56. Dahl, R. H., Zhang, F., Alonso-Gutierrez, J., Baidoo, E., Batth, T. S., Redding-Johanson, A. M., Petzold, C. J., Mukhopadhyay, A., Lee, T. S., Adams, P. D., and Keasling, J. D. (2013) Engineering dynamic pathway regulation using stress-response promoters, *Nat Biotechnol 31*, 1039.

57. Park, M., Tsai, S. L., and Chen, W. (2013) Microbial Biosensors: Engineered Microorganisms as the Sensing Machinery, *Sensors-Basel 13*, 5777-5795.

58. Amaro, F., Turkewitz, A. P., Martin-Gonzalez, A., and Gutierrez, J. C. (2014) Functional GFP-metallothionein fusion protein from Tetrahymena thermophila: a potential whole-cell

biosensor for monitoring heavy metal pollution and a cell model to study metallothionein overproduction effects, *Biometals 27*, 195-205.

59. Siedler, S., Khatri, N. K., Zsohar, A., Kjaerbolling, I., Vogt, M., Hammar, P., Nielsen, C. F., Marienhagen, J., Sommer, M., and Joensson, H. N. (2017) Development of a bacterial biosensor for rapid screening of yeast p-coumaric acid production, *ACS Synth Biol* DOI:10.1021/acssynbio.7b00009.

60. van der Meer, J. R., and Belkin, S. (2010) Where microbiology meets microengineering: design and applications of reporter bacteria, *Nat Rev Microbiol 8*, 511-522.

61. Xiong, D., Lu, S., Wu, J., Liang, C., Wang, W., Wang, W., Jin, J. M., and Tang, S. Y. (2017) Improving key enzyme activity in phenylpropanoid pathway with a designed biosensor, *Metab Eng 40*, 115-123.

62. van der Rest, M. E., Lange, C., and Molenaar, D. (1999) A heat shock following electroporation induces highly efficient transformation of Corynebacterium glutamicum with xenogeneic plasmid DNA, *Appl Microbiol Biotechnol 52*, 541-545.

63. Vinson, V. (2011) Inventive constructions using biobricks, *Science 331*, 30-30.

64. Marienhagen, J., and Eggeling, L. (2008) Metabolic Function of *Corynebacterium glutamicum* Aminotransferases AlaT and AvtA and Impact on L-Valine Production, *Appl Environ Microb 74*, 7457-7462.

65. Olsen, R. A., and Bakken, L. R. (1987) Viability of Soil Bacteria - Optimization of Plate-Counting Technique and Comparison between Total Counts and Plate Counts within Different Size Groups, *Microb Ecol 13*, 59-74.

66. Fukushima, T., Hayakawa, T., Kawaguchi, M., Ogura, R., Inoue, Y., Morishita, K., and Miyazaki, K. (2005) PBS buffer solutions with different pH values can change porosity of DNA-chitosan complexes, *Dent Mater J 24*, 414-421.

67. Schafer, A., Tauch, A., Droste, N., Puhler, A., and Kalinowski, J. (1997) The *Corynebacterium glutamicum* cglIM gene encoding a 5-cytosine methyltransferase enzyme confers a specific DNA methylation pattern in an McrBC-deficient *Escherichia coli* strain, *Gene 203*, 95-101.

68. Tauch, A., Kirchner, O., Loffler, B., Gotker, S., Puhler, A., and Kalinowski, J. (2002) Efficient electrotransformation of C*orynebacterium diphtheriae* with a mini-replicon derived from the *Corynebacterium glutamicum* plasmid pGA1, *Curr Microbiol 45*, 362-367.

69. Rytter, J. V., Helmark, S., Chen, J., Lezyk, M. J., Solem, C., and Jensen, P. R. (2014) Synthetic promoter libraries for *Corynebacterium glutamicum*, *Appl Microbiol Biotechnol 98*, 2617-2623.

a) Table 1. Bacterial strains, plasmids and primers used in this study

Strains/plasmids/ Primers	Relevant characteristics	Source/reference/notes
Strains		
E. coli DH5α	F$^-$*endA1thi-1 recA1 relA1 gyrA96deoRΦ80dlac*Δ(*lacZ*) M15 Δ(*lacZYA-argF*)*U169hsdR17*(r_K^-, m_K^+) λ$^-$ *supE44 phoA*	Transgene
C. glutamicum RES167	Restriction-deficient mutant of *C. glutamicum* ATCC 13032, lacking the restriction-modification locus and a large fragment of CGP3 prophage	University of Bielefeld [67, 68]
ΔaroK	*C. glutamicum* RES167 with deletion of a fragment of DNA encoding for *aroK*	[21]
GBD9	*ΔaroK* harboring pGBD9	This study
GBTDE	*ΔaroK* harboring pGBTDE	[21]
SENSOR	RES167 harboring pSA	This study
WCSENSOR	RES167 harboring pWCSA	This study
LSA	*ΔaroK* harboring pSA	This study
MSA	GBD9 harboring pSA	This study
HSA	GBTDE harboring pSA	This study
RLIB	LSA harboring pRLIB	This study
TKTA	*ΔaroK* harboring pTKTA	This study
Plasmid		
pXMJ19	*C. glutamicum*/*E. coli* shuttle vector (Cam^r, P_{tac}, *lacI*^{q}, pBL1 *ori*$V_{C.glu.}$ pK18 *ori*$V_{E.\ coli.}$)	University of Bielefeld
pBiobrick19	Derived from pXMJ19 by replacing the expression cassette with Biobrick adapters	This study
pEC-XK99E	*C. glutamicum*/*E. coli* shuttle vector (Kan^R, P_{tac}, l*acI*^{q}, pGA1 per gene)	University of Bielefeld
pEC99-lacI^{q-}	Derived from pEC-XK99E by replacing the promoter P_{tac}, the *rrnB* T1T2 terminator and the *lacI*^{q} with Biobricks adapters	This study
pSA	pEC99-lacI^{q-} carrying *eGFP* gene under the control of the ShiR cognate promoter region	This study
pWCSA	pSA carrying the *shiA* gene controlled by constitutive promoter P_{4945}	This study
pGBD9	pBiobrick19 carrying a heterogeneous shikimate synthesis module	This study
pGBTDE	pXMJ19 carrying RBS-optimized shikimate synthesis module	[21]
pRLIB	pBiobrick19 carrying *tktA* gene with saturated RBS library	This study
pTKTA	pBiobrick19 carrying *tktA* gene with recognized strong RBS_u*	This study

pTE	pXMJ19 carrying *tktA-eGFP* fusion gene without RBS	This study
$pRBS_u$-TE	pXMJ19 carrying *tktA-eGFP* fusion gene controlled by RBS_u*	This study
$pRBS_{13}$-TE	pXMJ19 carrying *tktA-eGFP* fusion gene controlled by RBS_{13}*	This study
$pRBS_{22}$-TE	pXMJ19 carrying *tktA-eGFP* fusion gene controlled by RBS_{22}*	This study
$pRBS_{23}$-TE	pXMJ19 carrying *tktA-eGFP* fusion gene controlled by RBS_{23}*	This study
Primers	**Sequence**	
P_99-lacI^{q-}_F	CATGAATTCGAGCTCGGTACCCGGGGAT	This study
P_99-lacI^{q-}_R	CATGAATTCGTGTCAACGTAAATGCATGCCGCTTC	This study
P_ pB19_F	GCAGAATTCGCGGCCGCtTCTAGAG	This study
P_ pB19_R	GATGAATTCCTCAGGGCCAGGCGGTGAAGGGCAATC	This study

Sequence ID	**Sequence**	
shiA promoter region (ShiR cognate promoter region)	GCAGAATTCGCGGCCGCTTCTAGACAAAAGAGGCCTA AAAATTAGGGGGAAATTAGGTCTCAAACAGAGATTTTT TCAATTAGTTTTGTGGTGTTTTCACACGGCTTCACACT CTCAATAGTTTCTATTTACAAAGGTTAACGCCATAAAAG TGGCCTCCACTACATAATTAAGTCAAAATCTTACTTAAA GAATGTGGAATTGCGCATTTCTCTTACAAAGTGATCCG CCATATAGTTCATTCCATTGGTATCCAGCTCACAGTTTA GGTTCCAAACGGATAGCCACTTGACCTAAATACCCATT CCTTTGAGAGGGAATACGACTAGTAGCGGCCGCCTG CAGGCT	39
Synthesized constitutive promoter P_{4945}	TTGACAAATAAGGTTGTATGTGCTATAATGGACC	69
Terminator sequence	AGCTTGGCTGTTTTGGCGGATGAGAGAAGATTTTCAG CCTGATACAGATTAAATCAGAACGCAGAAGCGGTCTG ATAAAACAGAATTTGCCTGGCGGCAGTAGCGCGGTGG TCCCACCTGACCCCATGCCGAACTCAGAAGTGAAAC GCCGTAGCGCCGATGGTAGTGTGGGGTCTCCCCATG CGAGAGTAGGGAACTGCCAGGCATCAAATAAAACGAA AGGCTCAGTCGAAAGACTGGGCCTTTCGTTTTATCTG TTGTTTGTCGGTGAACGCTCTCCTGAGTAGGACAAAT CCGCCGGGAGCGGATTTGAACGTTGCGAAGCAACGG CCCGGAGGGTGGCGGGCAGGACGCCCGCCTCTACA AACTCT	21

*the sequence of each RBS is shown in Figure 6g.

Figure caption

Figure 1. Schematic diagram of shikimate pathway in *C. glutamicum*. GAP: glyceraldehyde-3-phosphate, PEP: phosphoenolpyruvate, E4P: erythrose-4-phosphate, DAHP: 3-deoxy-D-arabinoheptulosonate-7-phosphate, DHQ: 3-dehydroquinate, DHS: 3-dehydroshikimate, SA: shikimic acid, S3P: shikimate-3-phosphate, EPSP: 5-enolpyruvyl-shikimate 3-phosphate, CHA: chorismate, PCA: protocatechuate, QA: quinic acid; *aroG*: DAHP synthase, *aroB*: DHQ synthase, *aroD*: DHQ dehydratase, *aroE*: SA dehydrogenase, *aroK*: SA kinase, *aroA*: EPSP synthase, *aroC*: CHA synthase, *qsuB*: DHS dehydratase, *qsuD*: QA dehydrogenase, *tktA*: transketolase, TCA cycle: tricarboxylic acid cycle; Shikimate-accumulating strain Δ*aroK* was derived by disrupting the *arok* gene of *C. glutamicum* RES167. This figure was adapted from[21].

Figure 2. Construction and verification of the intracellular SA biosensor. (a, b) the schematic diagram of the biosensor. In panel a, ShiR binds to the promoter region and impedes the expression of the *eGFP* gene in the absence of SA. In panel b, SA binds to ShiR and causes a protein conformational change, which initiates the synthesis of eGFP and generates fluorescence signals in *C. glutamicum*. (c, d) the confocal laser scanning microscopic images of non-SA-accumulating strain SENSOR (c) and SA-accumulating strain LSA (d). The *shiR* on the chromosome expressed constitutively in both strains, while SA only accumulated in LSA. The LSA cells displayed much stronger fluorescence in comparison to SENSOR cells after incubation for 24 hours.

Figure 3. The dose response of the biosensor-derived RFI to the intracellular SA concentrations during the fermentation of the HSA strain. (a) The changing curves of the RFI and the intracellular SA concentrations over time. The SA synthesis module pGBTDE was induced with IPTG for overexpression after the HSA cells were cultured to a late log phase, and the time point when 1mM IPTG was added to the culture was recognized as induction time 0; Circle: RFI (FI/OD_{600nm}), triangle: intracellular SA concentration (fmole/cell). (b) The linear correlation between RFIs and intracellular SA. The regression analysis revealed that the RFI was linearly respond to the intracellular SA concentration with one-hour lag, R^2=0.92.

Figure 4. Production (a) and monitoring (b) of the SA titer with the *C. glutamicum* strains LSA (circle), MSA (triangle) and HSA (square). In panel a, the time point when IPTG was added to the culture was recognized as fermentation time 0; In panel b, the solid line indicates the linear response of biosensor-derived RFI to the SA titer; (R_1^2=0.97, R_2^2=0.96, R_3^2=0.91).

Figure 5. Cell sorting of the *C. glutamicum* HSA and LSA mixed culture using flow cytometry. The contour plots (a) and histogram (b) of the SSC signal and the eGFP fluorescence. In panel a, the sorting gate is framed by a trapezoid to separate cells with the top 50% highest fluorescence from population II.

Figure 6. Flow diagram of the biosensor-based screening of the *tktA* RBS library and selection of high-yield *C. glutamicum* strain at the single-cell level with FACS. (a-d) The trapezoidal gate indicates the positive threshold. Cells distributed on the right side of the gate were considered to be fluorescence positive. The rectangle gate

indicates the sorting gate. (a) FACS of the LSA strain, used as a negative control. The positive rate for the control strain was set at 0%. (b) First-round pre-sorting of RLIB cells. The positive rate was 6.4% and the top 20% of the positive cells were collected. (c) Second-round pre-sorting of RLIB cells collected from the first-round of pre-sorting. A total of 26.5% of counted cells were positive, of which the top 10% cells were collected. (d) Final-round single-cell sorting of RLIB cells derived from the second-round pre-sorting. Approximately 46% of the cells were fluorescence positive, and the top 5% of positive cells were targeted for single-cell separation in a 96-well plate. (e) The fluorescence screening of sorted cells with a microplate reader. The FIs were exhibited using color gradation chart. The FI was proportional to the intensity of color. (f) Strains 13, 22 and 23 were selected for further fermentation in 500-mL flasks. The SA titer of each strain after 48-hour fermentation was exhibited in the bar chart; the strength of each RBS sequence, characterized using the RFI of TktA-eGFP fusion after induction for 27 hours, was shown in the line chart. (g) The RBS sequences in each strain are indicated.

Figure 7. Construction of the pWCSA plasmid by insertion of a *shiA* expression cassette into pSA plasmid.

Figure 8. The response of whole-cell SA biosensor to SA concentrations in culture medium. (a) The RFI of WCSENSOR cells logarithmically correlated with extracellular SA concentration from 0 to 500 mM (R_1^2=0.94); while from 0-100 mM, the RFI and extracellular SA had a linear correlation trend as shown in the enlarged figure at the lower right corner (R_2^2=0.85). (b) The linear detection range of the whole-cell

biosensor for SA was between 1 and 100 mM (R_3^2=0.99).

Figure 1.

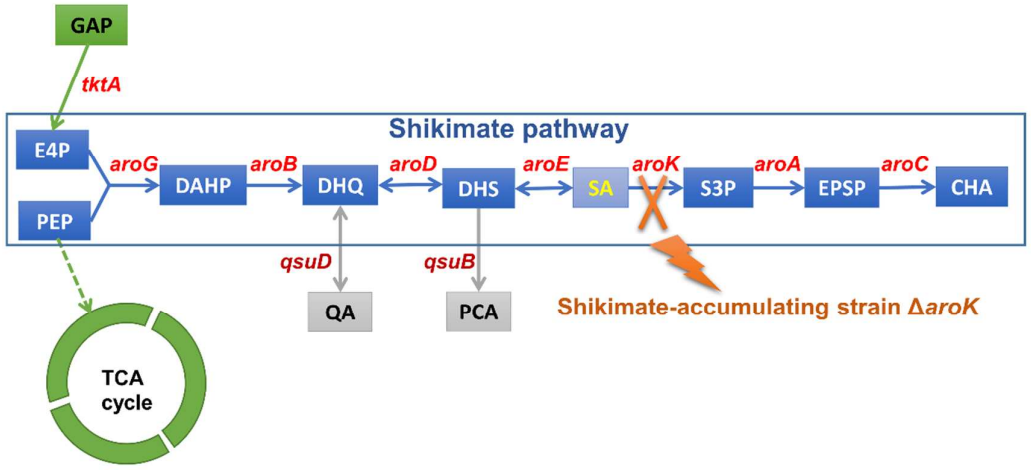
GAP
tktA
Shikimate pathway
E4P
PEP
aroG
DAHP
aroB
DHQ
aroD
DHS
aroE
SA
aroK
S3P
aroA
EPSP
aroC
CHA
qsuD
QA
qsuB
PCA
TCA cycle
Shikimate-accumulating strain ΔaroK

763 Figure 2.

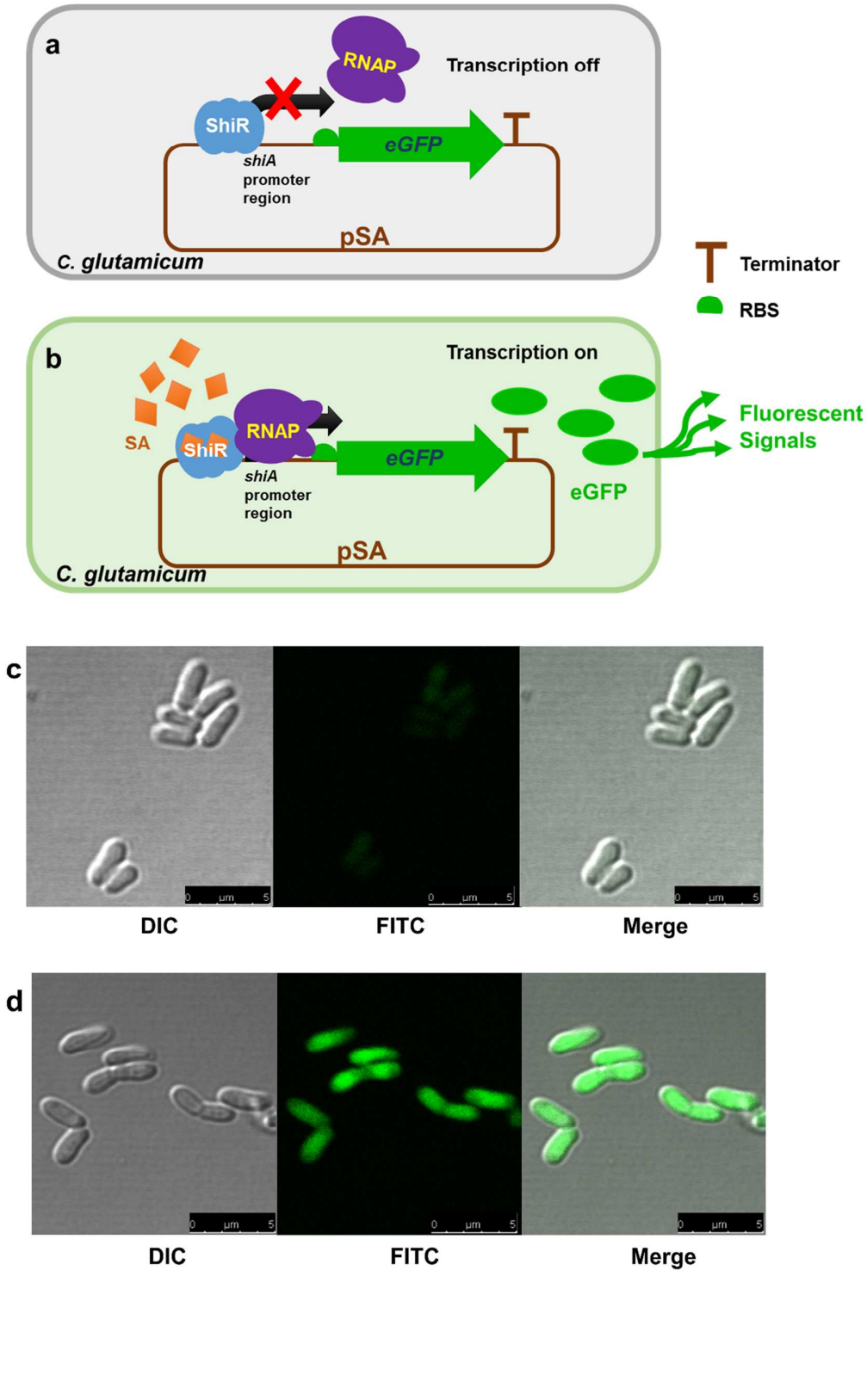

764

765

Figure 3.

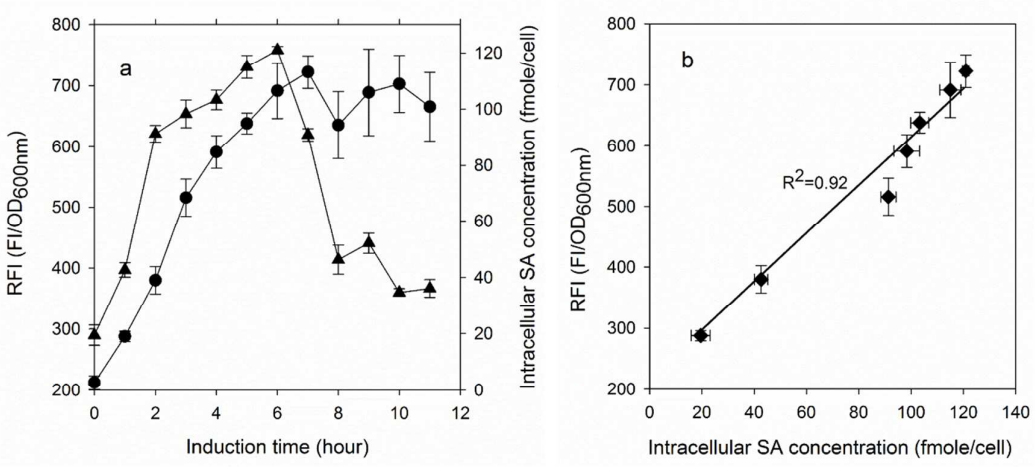

Figure 4.

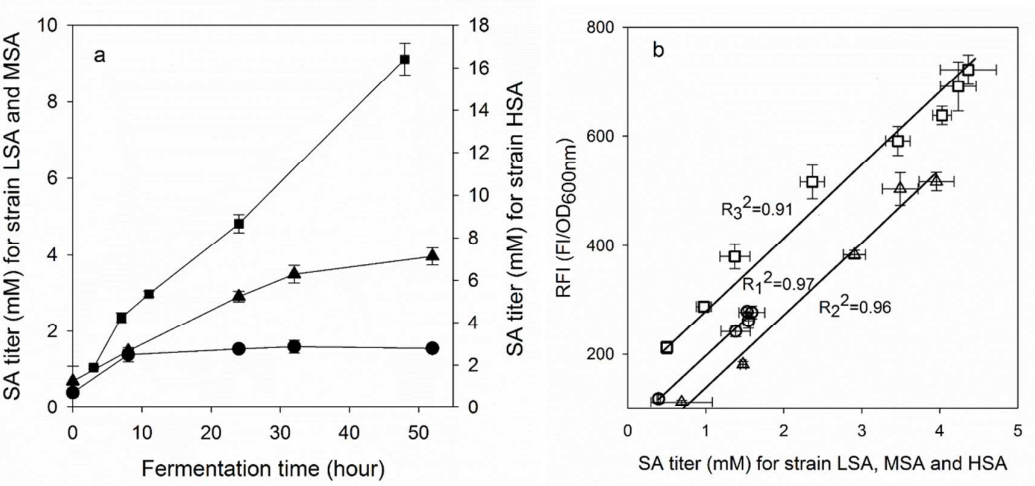

Figure 5.

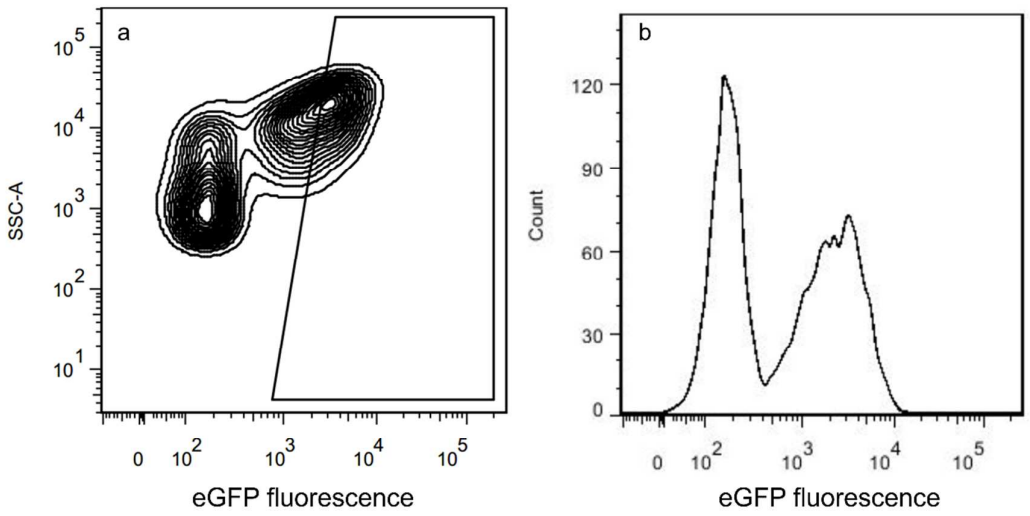

Figure 6.

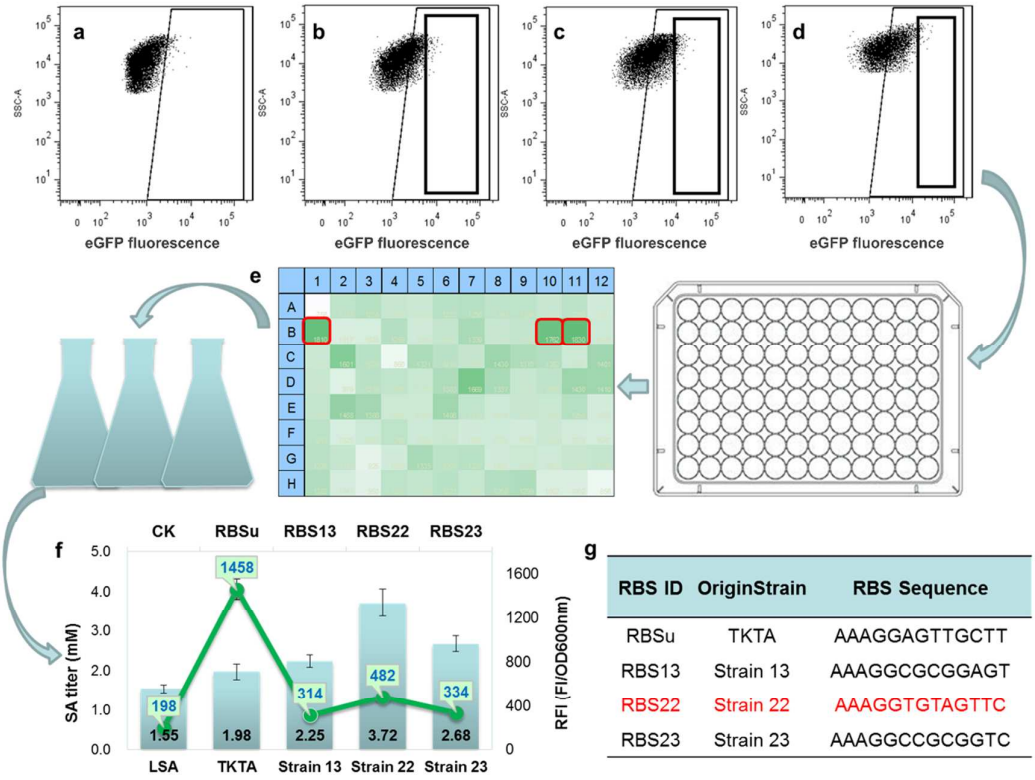

RBS ID	OriginStrain	RBS Sequence
RBSu	TKTA	AAAGGAGTTGCTT
RBS13	Strain 13	AAAGGCGCGGAGT
RBS22	Strain 22	AAAGGTGTAGTTC
RBS23	Strain 23	AAAGGCCGCGGTC

Figure 7.

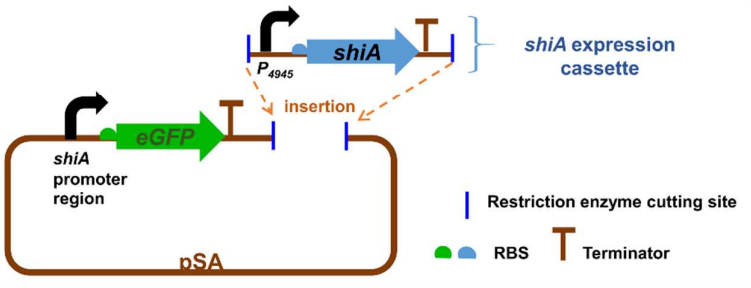

Figure 8.

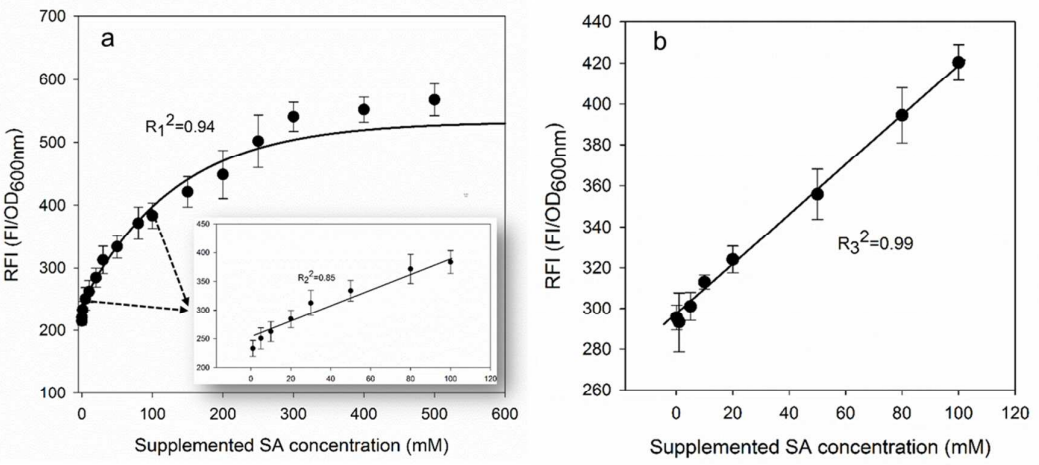

New intracellular shikimic acid biosensor for monitoring shikimate synthesis in *Corynebacterium glutamicum*

Chang Liu[1, 2], Bo Zhang[1, 3], Yi-Ming Liu[1], Ke-Qian Yang[1†], Shuang-Jiang Liu[1*]

[*]Correspondence: liusj@im.ac.cn

[†]Co-correspondence, deceased March 21st, 2017

[1]State Key Laboratory of Microbial Resources, Institute of Microbiology,

Chinese Academy of Sciences, West Beichen Road No.1, 100101 Beijing, PR China.

[2]University of Chinese Academy of Sciences, 100101 Beijing, PR China.

[3]Zhejiang University of Technology, 310014 Hangzhou, PR China.

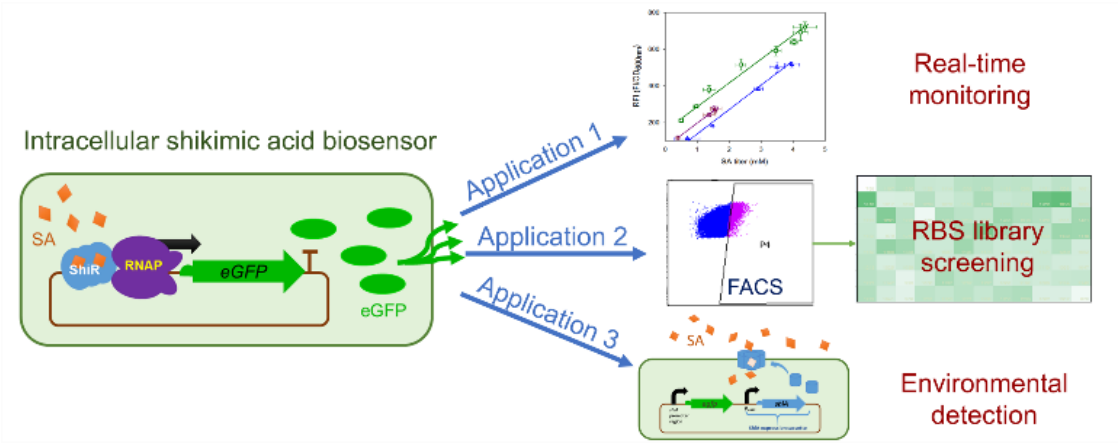
Intracellular shikimic acid biosensor
SA
ShiR
RNAP
eGFP
eGFP
Application 1
Application 2
Application 3
Real-time monitoring
FACS
RBS library screening
SA
Environmental detection